Numerical Simulations Demonstrate Safe Vitrification and Warming of Embryos Using the Rapid-i™ Device

Yury A. Tarakanov[*1], Björn O. J. Johansson[1,2], Hans J. Lehmann[2] and S. Peter Apell[1]

[1]Department of Applied Physics, Chalmers University of Technology, SE-412 96, Gothenburg, Sweden
[2]Vitrolife Sweden AB, Box 9080, SE-400 92, Gothenburg, Sweden
*Corresponding author. Address: Dept. of Applied Physics, Chalmers University of Technology, SE-412 96, Gothenburg, Sweden, e-mail: tarakano@chalmers.se

Abstract: During cryopreservation of human embryos, ice crystal formation in the embryos or in surrounding media may cause cryodamage to them and can be lethal. A strategy to avoid this is the vitrification procedure when the embryo and the surrounding medium undergo the transition to glassy state rather than a crystalline one during cooling. Similarly, recrystallization in the embryo or the medium must be avoided during the warming process. The necessary conditions for this are rapid cooling and warming rates.

We assess the cooling and warming rates in the Rapid-i™ device for vitrification and cryostorage of human embryos from Vitrolife Sweden AB with help of numerical simulations. We demonstrate that the fast cooling and warming rates necessary for safe vitrification and warming are achieved in the device. We also determine safe margins for the warming procedure.

Keywords: cryopreservation, vitrification, Rapid-i, cooling rate, warming rate

1. Introduction

Assisted reproductive technology (ART) is a science intensive technology to achieve pregnancy by artificial or partially artificial means. One of the challenges in ART is cryopreservation of human embryos with high survival rates. This is commonly achieved by freezing the embryos to cryogenic temperatures. During the freezing process, cryoinjuries caused by ice crystal formation in and around living cells may severely limit the embryos' survival rate. To avoid this, the embryo must be dehydrated with high concentrations of cryoprotectants and subjected to rapid cooling in order to achieve vitrification – a transition of the liquids in and around the embryo to a glass state rather than the crystalline one. When the embryo is warmed up before transfer to the uterus, recrystallization may occur at temperatures above the devitrification temperature, which is equally lethal for it; thus, high warming rates are required to avoid ice crystal formation during warming.

It is commonly assumed that the cooling process has a stronger influence on the survival of embryos than the warming one. Consequently, biomedical devices for vitrification and cryostorage are usually designed to maximize the cooling rate. A variety of devices have been developed to achieve fast cooling rates >10000 °C/min; some examples are nylon mesh [1], open-pulled straw [2], cryotops [3] and VitroLoop [4]. However, in a recent study Seki et al. [5] have clearly demonstrated that quick warming rates have a much higher relative importance for the survival of embryos than quick cooling rates. It has been shown that provided the warming rate is high (around 3000 °C/min), a high survival rate is achieved even at a slow freezing rate 200 °C/min, (while 500 °C/min is commonly accepted as a lower limit). This suggests that the vitrification devices should primarily be designed so as to ensure a quick warming.

In many devices, fast cooling rate is achieved by reducing the dimensions of the part which contains the vitrification solution with an embryo suspended in it, or/and by providing a direct contact between the vitrification solution and liquid nitrogen (LN_2) during vitrification. However, there is a concern that certain microorganisms can survive in LN_2 and infect the embryo; moreover, devices with small dimensions require extra precision in handling and are easier to destroy.

Increased device dimensions can benefit in terms of simplicity of manufacturing and operation and in terms of device durability, at a cost of lowered cooling rates. Still, the quick warming rate should be ensured to achieve high survival rates. In this study, we assess a device for vitrification, cryostorage and warming of human embryos, the Rapid-i™ from Vitrolife Sweden AB, that combines these advantages.

During clinical testing of the Rapid-i, high survival rates had been shown for human and mouse embryos. In this study, we have assessed the cooling and warming rates in the device; the information that is required to further ensure that no cryodamages are inflicted to embryos during operation. Measurement of these rates would require complicated and expensive experiments; on the contrary, numerical modeling offers a quick and reliable way to obtain them.

We have performed numerical modeling of vitrification and warming procedures using the Rapid-i™ device with help of COMSOL Multiphysics 3.5a. We have assessed the cooling and warming rates in the device and have shown that the warming rate is very high, while the cooling rate is well above the lower limit – thus, we have demonstrated that the device meets general requirements to vitrification devices.

The article is organized as follows. First, we describe the Rapid-i™ device and how it is used for vitrification and warming procedures. Then, we describe the modeling of the device: we present the model geometries we have used, write down the main equations of the heat transfer and list the material parameters. We also describe how the cooling and the warming rates have been extracted from the modeling results. We proceed with presenting the results of the simulations and finish with conclusions.

2. Modeling

2.1 The Rapid-i™ device

A schematic drawing of a Rapid-i™ device is shown in Figure 1. The device consists of a 77 millimeters (mm) long and 2 mm thick cylindrical stick ("Rapid-i stick") with a 3 mm long flattened part at the tip (a "holder" for the embryo) and a straw with inner and outer diameters of 2.7 and 3.3 mm, respectively, which is sealed at the bottom. The stick is made of polymethyl methacrylate (PMMA) and the straw of polyvinyl chloride (PVC). A drop of vitrification solution [6] with an embryo suspended in it is placed into a small reach-through hole on the holder. We will refer to the vitrification solution with the embryo in it as a "drop" in what follows.
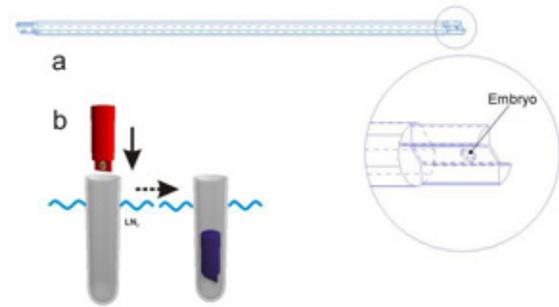
Figure 1. (a) A drawing of the Rapid-i stick. The inset shows a detailed view of the holder with a hole for placing the drop of vitrification solution with an embryo. (b) A schematic illustration of the open straw vitrification procedure.

The vitrification procedure can be performed in two ways. The "open straw" method comprises pre-freezing the straw by immersing it into LN_2 bath and then dropping a stick with a drop on it into the straw, as illustrated in Figure 1a. The straw is then sealed with the stick inside and placed in cryostorage. The "sealed straw" method consists in placing the stick with the drop into the straw, sealing it and then immersing it into LN_2.

In order to inseminate a stored embryo, it first has to be first warmed to room temperature. The warming procedure consists in cutting the straw at the top, extracting the stick with a vitrified drop and quickly placing it into the warming medium [6] which has a temperature T_{WM}=35°C. A direct contact between the warming medium and the drop is achieved which increases the warming rate. During the warming procedure, it is important to minimize the time during which the stick is exposed to air, because air provides slow warming possibly leading to ice formation in the drop and damage to the embryo.

2.2 The models and the model geometries

In order to simulate the vitrification and warming procedures of the Rapid-i™ device and to assess the cooling and warming rates, we have built up 6 models in total, 3 for the vitrification procedures and 3 for the warming ones.

The model geometries, built up in COMSOL Multiphysics 3.5a, are shown in Figure 2. All geometries except one have mirror symmetries with respect to the x=0 and y=0 planes (the axis of the Rapid-i stick coincides with the z-axis),

which allowed us to simplify the geometries in the computational models, as illustrated in Figure 2.
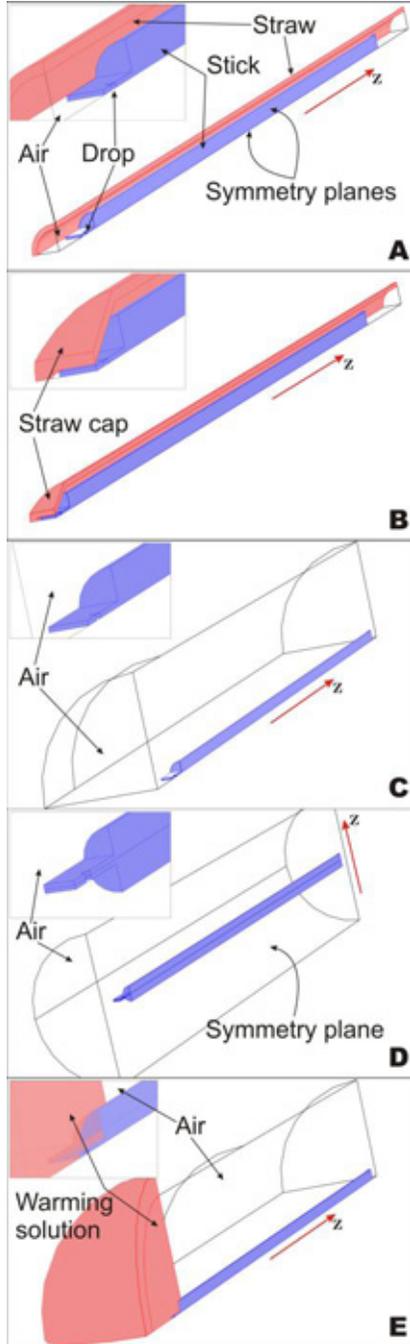
Figure 2. The COMSOL Multiphysics models used for simulation of vitrification and warming of embryos using the Rapid-i™ device. The insets zoom in on the holder part of the Rapid-i stick.

Model 1 addresses the dropping of the stick into the straw. The geometry used in this model is shown in Figure 2A. The stick with the drop on it are represented as non-moving domains in moving coordinate system, i.e. instead of the stick falling down with velocity $v_z = -gt$ (where g=9.8 m/s^2 is the gravitational constant and t is time), the air and the straw were modeled as moving upwards with the velocity $v_z = gt$ opposite to the one the stick would have.

Models 2 and 3 are used to simulate the cooling of the stick which has reached the sealed bottom of the straw and is not moving. These models use the same model geometry (shown in Figure 2B); the only difference is that the air is free to flow in and out through the top opening of the straw in model 2 (the "open straw" procedure) while in model 3 that opening is sealed (the "sealed straw" procedure).

Models 4 and 5 address the heat exchange between the stick with a vitrified drop on it and the air at room temperature. In model 4, the stick is positioned vertically (Figure 2C), while in model 5 it is held horizontally so that the geometry can be reduced by only one half, as shown in Figure 2D. The infinite air domains in these geometries are truncated to cylinders 20 millimeters in diameter coaxial with the stick. We have insured that these domains are big enough that the artificial air boundaries do not influence the simulation results.

Finally, Figure 2E shows the geometry of model 6, used for modeling the warming of the Rapid-i in the warming solution. The air and warming solution domains are truncated but still big enough to minimize the influence of the outer boundaries on the warming process.

2.3 The equations of the heat transfer

The heat exchange in the system is described by the heat transfer equation

$$\rho C_p \frac{\partial T}{\partial t} + \nabla \cdot \left(-k\nabla T \right) = -\rho C_p \vec{u} \cdot \nabla T, \quad 1$$

where T is absolute temperature, ρ is the density, C_p the specific heat capacity at constant pressure, k the thermal conductivity and $\vec{u}$ the velocity of the medium. The boundary conditions for the temperature are

- Fixed temperature $T=T_{ext}$ on the outer surface of the straw. The external

temperature T_{ext} is equal to the temperature of LN_2 $T_{LN_2} = -196$ °C below the LN_2 surface and to the room temperature $T_{room}=19$ °C above it.

- Fixed temperature T_{room} on the open boundaries through which air is expected to flow into the computational domain (upper and side air boundaries in the warming models 4-6), as well as on the sealed top of the straw in model 3.

- Fixed temperature $T=T_{WM}$ on the exterior boundaries of the warming medium in model 6.

- Symmetry $\vec{n} \cdot k\nabla T = 0$ ($\vec{n}$ is a unit vector normal to a boundary oriented in outward direction) on all boundaries on the symmetry planes in all models.

- Convective heat flux $\vec{n} \cdot k\nabla T = 0$ on the boundaries through which the air is expected to leave the computational domain (these are the top openings of the straw in models 1 and 2, bottom air boundaries in models 4 and 5, and side air boundaries above the surface of the warming medium in model 6).

- Continuity $\vec{n}_l \cdot k_l\nabla T_l = -\vec{n}_r \cdot k_r\nabla T_r$ (indices l and r denote the quantities in the domains to the left and right of the interface, and $\vec{n}_l = -\vec{n}_r$) on all interior boundaries in the model.

The initial temperatures of different components of the models, which serve as initial conditions for Eq. 1, are collected in Table 1.

The velocity field $\vec{u}$, which enters the right-hand side of Eq.1 and describes the convective heat transfer, is nonzero only in the straw in model 1, where it is prescribed to be $\vec{u} = -gt\hat{z}$, and in the air domain, where it is obtained by solving the weakly compressible Navier-Stokes equations

$$\frac{\partial \rho}{\partial t} + \nabla \cdot \left(\rho\vec{u} \right) = 0$$

$$\rho\frac{\partial \vec{u}}{\partial t} + \rho\vec{u} \cdot \nabla\vec{u} = -\nabla p +$$

$$+\nabla \cdot \left(\eta \left(\nabla\vec{u} + \nabla\vec{u}^T \right) - \frac{2}{3}\eta \left(\nabla \cdot \vec{u} \right) I \right) + \vec{F},$$

$$2$$

where p is the dynamic air pressure, η the dynamic viscosity of air, and $\vec{F}$ the volume force exerted on it. This force is the buoyancy force which appears due to thermal expansion of air,

$$\vec{F} = \hat{z}F_z = -g\hat{z} \left(\rho - \rho_0 \right), \qquad 3$$

where $\rho_0=1.19$ kg/m^3 the density of air at room temperature and atmospheric pressure. The density of air is calculated as a function of both temperature and pressure according to the ideal gas law

$$\rho = \frac{M}{R}\frac{P}{T}, \qquad 4$$

where $M=29$ g/mol is the molar mass of air, $R=8.31$ J·K^{-1}·mol^{-1} the universal gas constant and $P=p+10^5$ Pa the absolute (dynamic plus atmospheric) pressure.

We have neglected the motion of the warming medium because its dynamic viscosity is very high (20 Pa·s at room temperature).

The boundary conditions for the Navier-Stokes equations are:

- Wall, $\vec{u} = 0$, on the interface between the air and the Rapid-i stick (and the drop) in all models, on the interface between the air and the straw in models 2 and 3, and on the interface between the air and the warming medium in model 6.

- Moving wall, $\vec{u} = -gt\hat{z}$, on the interface between the air and the straw in model 1.

- Symmetry boundary,

$$\begin{cases} \vec{u} \cdot \vec{n} = 0 \\ \vec{t} \cdot \left(-p\vec{I} + \eta \left(\nabla\vec{u} + \nabla\vec{u}^T \right) \right)\vec{n} = 0 \end{cases}$$

where $\vec{t}$ is a vector of unit length tangential to the boundary, on the air boundaries on the symmetry planes.

- Inlet with a prescribed velocity, $\vec{u} = -gt\hat{z}$, on the bottom boundary of air (the bottom opening of the straw) in model 1.

- Inlet (zero pressure, no viscous stress)

$$\begin{cases} \eta \left(\nabla\vec{u} + \nabla\vec{u}^T \right) \cdot \vec{n} = 0 \\ p = 0 \end{cases},$$

on the exterior boundaries through which the air is expected to enter the computational domain.

- Outlet, zero normal stress

$$\left[-p\vec{I} + \eta\left(\nabla\vec{u} + \left(\nabla\vec{u} \right)^{T} \right) \right] \cdot \vec{n} = 0$$

on the exterior boundaries through which the air is expected to leave the computational domain.

The initial conditions are zero dynamic pressure (atmospheric absolute pressure) and zero velocity field in all models.

Table 1. The initial temperatures of the components in the models.

Model	Stick	Drop	Air	Straw	Warming medium
1	T_{room}	T_{room}	T_{room}	T_{ext}	-
2	T_{room}	T_{room}	T_{ext}	T_{ext}	-
3	T_{room}	T_{room}	T_{room}	T_{room}	-
4	T_{LN_2}	T_{LN_2}	T_{room}	-	-
5	T_{LN_2}	T_{LN_2}	T_{room}	-	-
6	T_{LN_2}	T_{LN_2}	T_{room}	-	T_{WM}

2.4 Material properties

The material properties of PVC, PMMA, vitrification and warming media which enter the heat transfer equation, are given in Table 2.

The thermodynamic properties of PVC and PMMA are to a high degree temperature independent. Their values have been taken from the COMSOL Materials Library.

The vitrification and warming media are multicomponent solutions whose thermodynamic parameters have not been measured; the values of the parameters given in Table 2 are calculated as weighted averages of the respective values for their components at 25°C; the latter are taken from [7].

We have neglected the temperature dependence of the properties of vitrification and warming media; we argue that this does not considerably influence the accuracy of the

cooling and warming rates because (i) the volume of vitrification solution (~10 nanoliters) is very small compared to the volume of the Rapid-i stick, so the cooling/warming dynamics on the device level are primarily influenced by the thermodynamic properties of the latter, and (ii) only a thin layer of the warming solution close to the stick is cooled down considerably below T_{WM}.

Table 2. The properties of PMMA, PVC and vitrification and warming media.

Material	Density, kg/m^3	Heat capacity, J/(kg·K)	Thermal conductivity, W/(m·K)
PMMA	1190	1420	0.19
PVC	1760	1047	0.10
Vitrification medium	1255	1657	0.20
Warming medium	1581	1255	0.28

On the contrary, the parameters of air, which change drastically with temperature, have a major effect on the heat exchange in the device. In order to maintain good accuracy in the modeling, we have used the temperature and pressure dependent air density (calculated using Eq.4) and the specific heat capacity, thermal conductivity and dynamic viscosity interpolated from experimental data in wide temperature ranges. The values outside the ranges, if needed, have been calculated by linear extrapolation. The temperature ranges and the literature sources for the experimental data are listed in Table 3.

Table 3. Literature sources and temperature ranges for the thermodynamic properties of air.

Name	Temperature range (K)	Source
C_p	82-360	Lemmon et al. [8]
k	85-400	Kadoya et al. [9]
η	85-400	Kadoya et al. [9]

Although air liquefaction takes place at -194 °C, just above the boiling temperature of LN_2, we do not take it into account. We note that taking the process of liquefaction/vaporization of the air into models would be complicated and the effect would be only a slight increase of the cooling rates (due to vaporization of the liquid air at the beginning of the cooling process) and no considerable change in warming rates in the interesting temperature range.

2.5 Modeling in COMSOL Multiphysics

We have used COMSOL Multiphysics 3.5a to perform the modeling of the heat transfer dynamics in the models described above. The finite element scheme has been used in order to solve the time-dependent heat transfer equation (1) and the Navier-Stokes equations (2) and to obtain the temperature distribution in the system as a function of time.

The cooling and warming rates for the embryo in the vitrification solution are the quantities of the major interest in this study. We have defined the "embryo temperature" T_{emb} as the temperature of the center of the drop of vitrification medium. Then, the "instant" embryo cooling/warming rate is defined as

$$R_{C(W)} = \left| \frac{dT_{emb}}{dt} \right| \qquad 5$$

(the cooling rate R_C applies to the vitrification process and the warming rate R_W to the warming one). These rates can be very high in the beginning of the vitrification and warming processes when the temperature difference between the drop and the surrounding media is high, but inevitably decrease as the temperatures equalize. In order to quantify the cooling and warming efficiency of the device in the wide temperature range, we introduce average cooling and warming rates which tell us how quickly the embryo temperature changes between 0°C and -130°C (which is the temperature range where the phase transitions in the embryo and vitrification medium relevant to vitrification and ice crystal formation occur):

$$R_{C(W)}^{aver} = \left| \frac{130}{t_{0^oC} - t_{-130^oC}} \right|, \qquad 6$$

where t_{0^oC} and t_{-130^oC} are the times at which the embryo temperature is equal to 0 °C and -130 °C, respectively.

The last quantity of interest is the maximum time the cold Rapid-i stick can be exposed to air before inserting it into the warming solution during the warming procedure. We further refer to it as "maximum air exposure time" t_{exp} and calculate it as the time required for the embryo temperature to reach -150°C in the models dealing with warming in air (models 4 and 5).

In order to achieve a convergence in the models with strong initial temperature gradients, we have implemented a gradual increase of the heat conduction through the air interfaces at initial times. This does not influence the behavior of the system in the interesting temperature range, but results in spikes in the warming rates at lowest temperatures in Figures 4 and 6. The method also introduces a small time delay in the onset of cooling and warming which is taken into account when calculating t_{exp}.

3. Results

3.1 Vitrification

The simulation of the dropping of the stick with the embryo into the straw has shown that the temperature of the stick and the vitrification solution does not change more than a fraction of a degree centigrade during the time it takes the stick to reach the straw bottom. This negligible cooling, which is a result of very short time (~0.1 second) it takes the stick to reach the bottom of the straw, implies that the meaningful cooling dynamics can be obtained from a model where the stick is already located at the bottom of the straw (model 2), and the room temperature is a good initial condition for the stick and the drop in that model.

Figure 3 shows the vitrification dynamics in Rapid-i for both open straw and sealed straw vitrification procedures. Embryo temperature versus time and embryo freezing rate versus temperature are depicted in Figure 3A and 3B, respectively.

It is apparent from the data that the open straw provides slightly quicker initial cooling. This is due to the fact that the straw and air inside it have already been cooled down by the time the stick is inserted, while in the sealed-

straw procedure, the straw and air in it are initially warm. In spite of this, the average embryo cooling rates are found to be practically identical, 1220 °C/min.

We conclude that the cooling rates obtained in both procedures exceed those required for a safe vitrification [5], and the difference in the cooling rates between the two methods is negligible. However, the air pressure inside the sealed straw drops to ¼ of atmospheric during freezing which can affect the environment for the embryo.
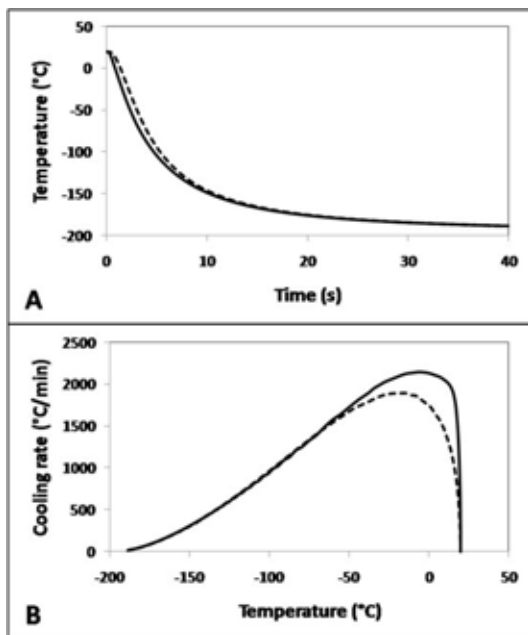
Figure 3. Embryo temperature against time (A) and embryo cooling rate against temperature (B) in the Rapid-i for open straw and sealed straw vitrification procedures (solid and dashed lines, respectively).

3.2 Warming

The dynamics of the warming of embryo in the air is shown in Figure 4. The calculated embryo temperature is plotted against time and the embryo warming rate versus its temperature for the cases when the stick is held vertically (model 4) and horizontally (model 5).

The modeling demonstrates the danger of too long exposure of the vitrified embryo to air. The warming rates in both cases are too low which most probably will lead to ice formation in the devitrified solution and consequently a cryodamage of embryo. The maximum exposure

times for the stick held horizontally and vertically, $t_{max,h}$ and $t_{max,v}$, are found to be 2.25 seconds and 7.2 seconds, respectively, see Figure 4A. A lower warming rate in the latter case means that the critical temperature -150 °C is passed at later times.
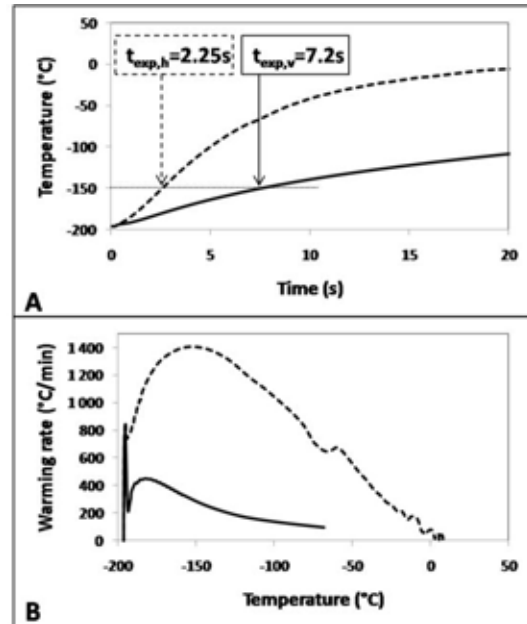
Figure 4. Embryo temperature against time (A) and embryo warming rate against temperature (B) in Rapid-i stick when it is exposed to air at room temperature. The stick is held vertically (solid lines) and horizontally (dashed lines).

To explain why the warming rates are so different for the two cases, we draw the air flow directions and the air temperature distribution in the vicinity of the drop in Figure 5. If the stick is held vertically, the air is descending around it and cools down before going into contact with the holder; moreover, the narrowing of the stick at holder creates a back step and impedes the convective warming. On the contrary, the holder is reached by the warm air in the opposite case, which makes the convective warming more efficient and increases the warming rate.

Finally, Figure 6 shows the embryo temperature and warming rate for the Rapid-i stick warmed up in a warming solution. Due to the high thermal conductivity of the solution, the warming rate is two orders of magnitude higher compared to warming in air and much higher than the rate required for devitrification of the

embryo without ice formation. The instant warming rate reaches as much as 50000 °C/min and the average warming rate is found to be 7700 °C/min.
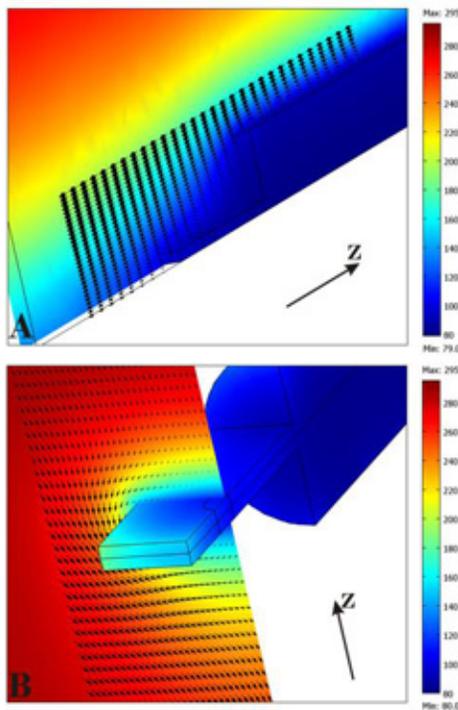
Figure 5. Illustration of the convective warming of the Rapid-i stick held vertically (A) or horizontally (B). The velocity field in a plane cutting through the vitrification solution drop is shown by arrows, and the temperature of the stick and the air is given by color code. The plots are made at t=2s. The convective heating of the drop is more efficient in the horizontal configuration (B) where the warm air flows past it, while the air is cooled down by the stick before reaching the drop in the vertical one (A).

4. Conclusions

To conclude, we have modeled the vitrification and warming procedures using the Rapid-i™ device. We have demonstrated that the cooling and warming rates in the device are fast enough to ensure safe conditions for the embryo; while the average cooling rate for the vitrification procedure is 1220 °C/min, the average warming rate in the device immersed into warming solution is 7700 °C/min. Thus, the Rapid-i™ device meets the requirements for high cooling and warming rates required for avoiding cryodamages of embryos. By modeling

the warming of the device in air, we have seen that such warming is too slow and therefore is dangerous for the embyo. We have found the maximum times during which the cold Rapid-i stick can be exposed to air, which differ significantly depending on how the warmed stick is held. Based on the worst-case scenario (which takes place if the Rapid-i stick is held horizontally), the maximum time to transfer the embryo from the straw into the warming solution should be limited by 2 seconds.
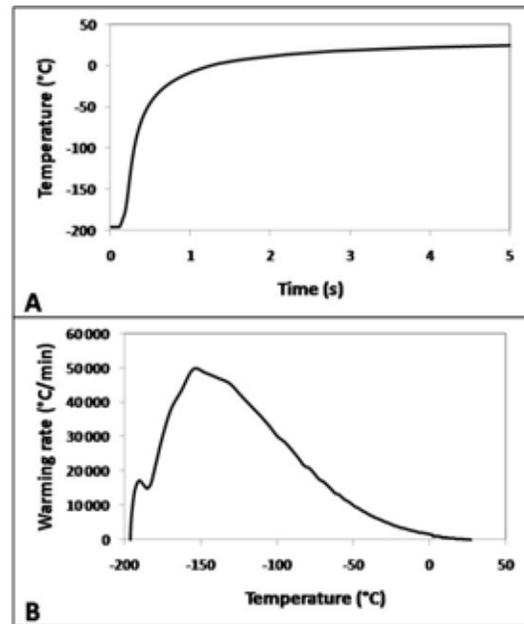
Figure 6. Embryo temperature against time (A) and embryo warming rate against temperature (B) in Rapid-i stick warmed in the warming solution.

In this study, we have used a simplification in a form of constant material parameters for the vitrification and warming media. Further studies should address the physical processes related to phase changes in the vitrification solution in connection to cooling or warming of the system, which will not only increase the precision of the obtained results but also give a valuable insight into the dynamic interplay of thermophysical and biological processes in the vitrification and warming of embryos.

5. References

1. H. Matsumoto, J.Y. Jiang, T. Tanaka, H. Sasada, E. Sato, "Vitrification of large quantities

of immature bovine oocytes using nylon mesh", *Cryobiology* **42**, 139-144 (2001)

2. G. Vajta, P.J. Booth, P. Holm, T. Greve, H. Callesen, "Successful vitrification of early stage bovine in vitro produced embryos with the open pulled straw (OPS) method", *Cryo-Letters* **18**, 191-195 (1997)

3. M. Kuwayama, "Highly efficient vitrification for cryopreservation of human oocytes and embryos: the Cryotop method", *Theriogenology* **67**, 73-80 (2007)

4. M. Lane and D.K. Gardner, "Live births following vitrification of mouse oocytes using the VitroLoop", *Fertility and Sterility*, **74**, 3 (2000)

5. S. Seki and P. Mazur, "The dominance of warming rate over cooling rate in survival of mouse oocytes subjected to a vitrification procedure", *Cryobiology* **59**, 75-82 (2009)

6. The constituents and their concentrations in the vitrification and the warming solutions are properties of Vitrolife Sweden AB and are not given here.

7. CRC Handbook of Chemistry and Physics, 89th edition, CRC press LLC, 2008-2009.

8. E.W. Lemmon, R.T. Jacobsen, S.G. Penoncello and D.G. Friend, "Thermodynamic properties of air and mixtures of nitrogen, argon, and oxygen from 60 to 2000 K at pressures to 2000 MPa", *J. Phys. Chem. Ref. Data*, **29**, 3 (2000)

9. K. Kadoya, N. Matsunaga and A. Nagashima, "Viscosity and thermal conductivity of dry air in the gaseous phase", *J. Phys. Chem. Ref. Data*, **14**, 4 (1985)

6. Acknowledgements